An Allosteric Intramolecular PDZ−PDZ Interaction Modulates PTP-BL PDZ2 Binding Specificity†

Lieke C. J. van den Berk,‡ Elena Landi,§ Tine Walma,|| Geerten W. Vuister,|| Luciana Dente,§ and Wiljan J. A. J. Hendriks*,‡

Department of Cell Biology, Radboud University Nijmegen Medical Centre, and Protein Biophysics, Institute for Molecules and Materials, Radboud University Nijmegen, Nijmegen, The Netherlands, and Department of Biology, University of Pisa, Pisa, Italy

Received May 18, 2007; Revised Manuscript Received September 20, 2007

ABSTRACT: PDZ (acronym of the synapse-associated protein PSD-95/SAP90, the septate junction protein Discs-large, and the tight junction protein ZO-1) domains are abundant small globular protein interaction domains that mainly recognize the carboxyl termini of their target proteins. Detailed knowledge on PDZ domain binding specificity is a prerequisite for understanding the interaction networks they establish. We determined the binding preference of the five PDZ domains in the protein tyrosine phosphatase PTP-BL by screening a random C-terminal peptide λ phage display library. Interestingly, the potential of PDZ2 to interact with class III-type ligands was found to be modulated by the presence of PDZ1. Structural studies revealed a direct and specific interaction of PDZ1 with a surface on PDZ2 that is opposite the peptide binding groove. Long-range allosteric effects that cause structural changes in the PDZ2 peptide binding groove thus explain the altered PDZ2 binding preference. Our results experimentally corroborate that the molecular embedding of PDZ domains is an important determinant of their ligand binding specificity.

In cellular signaling networks, dynamic protein−protein interactions form the backbone of information flow, and the large number of specialized protein domains that mediate these contacts highlights their importance in signal transduction (*1*). The PDZ[1] domain (acronym of the synapse-associated protein PSD-95/SAP90, the septate junction protein Discs-large, and the tight junction protein ZO-1) is one of the most common protein interaction modules in metazoan genomes. It participates in a wide variety of signaling pathways and contributes to the protein sorting and transport machinery (*2*, *3*). PDZ domains adopt a compact globular fold comprising six β-strands, which form two antiparallel β-sheets stacked on top of each other, and two α-helices. They typically recognize short carboxyl-terminal peptide sequences in target proteins by β-sheet augmentation in a binding groove located between helix α2 and strand β2. It is well documented that in particular the ultimate (P^0) and antepenultimate (P^{-2}) amino acids in these canonical C-terminal targets are of crucial importance in determining PDZ domain affinity, and this has led to the definition of several different PDZ binding classes (*4*−*6*).

Many PDZ domain-containing proteins harbor multiple PDZ domains that are often arranged in closely linked groups. This renders the proteins capable of binding to several different transmembrane or intracellular partners at the same time, thus organizing multimeric complexes. For example, the large intracellular phosphotyrosine-specific phosphatase PTP-BL contains five PDZ domains, the second and third as well as the fourth and fifth of which are tandemly linked (*7*, *8*). Evidence is accumulating that intramolecular synergistic or allosteric effects may regulate PDZ domain binding potential (*9*−*11*), and for some PDZ domain tandems it has been shown that their target-binding preference differs from that of the PDZ domains separately (*12*−*14*). Also for PTP-BL synergistic effects on PDZ target peptide binding have been noted (*15*, *16*), and structural studies on the second PTP-BL PDZ domain (PDZ2) added proof for allosteric effects upon target peptide binding (*17*−*19*). Here, we report on the binding preferences of PTP-BL PDZ domains individually and in clusters. Our data reveal an allosteric regulation of the PTP-BL PDZ2 binding preference, through direct contact of PDZ1 with a PDZ2 surface area opposite the binding pocket. These findings disclose a novel PDZ−PDZ interaction that regulates PDZ binding specificity through an allosteric mechanism.

MATERIALS AND METHODS

Expression Plasmids. Bacterial expression plasmids pGEX-PDZ1, pGEX-PDZ2, pGEX-PDZ3, pGEX-PDZ4, pGEX-PDZ5, pGEX-PDZ1+2, pGEX-PDZ1+2ΔL, pGEX-PDZ4+5, and pGEX-PDZ2−5 were constructed by subcloning of PCR-generated PTP-BL cDNA fragments (spanning residue numbers 1078−1171, 1353−1449, 1489−1601, 1756−1855, 1853−1946, 1064−1501, 1080−1189 fused to 1352−1451, 1661−2021, and 1285−1978, respectively; numbers accord-

† This work was supported by the Dutch Organization for Earth and Life Sciences (NWO-ALW Grants 809-38-004 and 809-38-007), by FIRB Neuroscienze (Grant RBNE01 WY7P), by the AMBISEN Center, University of Pisa, by MIUR-PRIN (Grant 2006054104_002), and by the EC quality of life and management on living resources program (Grant QLG3-CT-01460). G.W.V. acknowledges funding by NWO-CW Grant 700.55.443.

* To whom correspondence should be addressed. Phone: +31-24-3614329. Fax: +31-24-3615317. E-mail: w.hendriks@ncmls.ru.nl.

‡ Radboud University Nijmegen Medical Centre.

§ Institute for Molecules and Materials, Radboud University Nijmegen.

|| University of Pisa.

[1] Abbreviations: PDZ, acronym of PSD-95/SAP90, Discs-large, and ZO-1; SPR, surface plasmon resonance; CRIB, acronym of Cdc42/Rac interactive binding.

10.1021/bi700954e CCC: $37.00
Published on Web 11/03/2007

ing to accession no. Q64512) in-frame into appropriate pGEX vectors. Primer and construction details are available from the authors upon request.

GST Fusion Protein Production and Purification. GST fusion proteins, expressed in *Escherichia coli* DH5α following transformation with pGEX-based constructs, were affinity-purified on glutathione−Sepharose 4B beads (Amersham Biosciences, England) as described (*20*). For surface plasmon resonance (SPR) purposes, GST fusion proteins were eluted from the beads using 10 mM reduced glutathione in 50 mM Tris−HCl, pH 8.0, and subsequently dialyzed against HBS (10 mM Hepes, pH 7.4, 150 mM NaCl, 3 mM EDTA, 0.005% surfactant P20; BR-1000-54, Biacore AB, Switzerland). For structural studies, GST-PDZ1 fusion protein was expressed in *E. coli* BL21 Codon Plus (DE3) RIL cells (Stratagene, California). The bacterial pellet was resuspended in PBS in the presence of 1 mM PMSF and Complete protease inhibitor (Roche, Mannheim, Germany) and sonified. Lysed bacteria were then centrifuged twice at 10 000 rpm at 4 °C for 30 min to remove cell debris. The supernatant was bound to glutathione−Sepharose 4B beads and washed with 0.1 M NaCl in 20 mM Tris−HCl, pH 8.0. Elution from the column was performed with 15 mM reduced glutathione in 50 mM Tris−HCl, pH 7.7. To remove the GST tag, 35 units of thrombin/mL was added for about 18 h at 25 °C. The mixture was passed over a Sephadex G75 size exclusion column at room temperature, and appropriate fractions were collected, pooled, and dialyzed against excess water overnight at 4 °C. Resulting PDZ1 protein was freeze-dried and stored at −80 °C until further use. Production and purification of ^{15}N-labeled His-tagged PDZ2 protein in *E. coli* BL21(DE3) cells has been described previously (*21*).

Phage Display Library Screening. Phage display experiments were performed as described before (*4*). In brief, a carboxyl-terminal nine amino acid random peptide library (with a complexity of 10^7 independent clones) displayed as capsid protein D fusions on bacteriophage λ (*4*) was screened by affinity selection over glutathione−Sepharose 4B beads coated with GST−PDZ fusion protein. Following extensive washes, adsorbed phages were propagated on BB4 bacteria by plate lysate, eluted, concentrated, and subjected to another panning cycle. After three successive panning cycles, individual phage clones were plaque-purified, and PCR-amplified inserts were sequenced.

Surface Plasmon Resonance. A Biacore 2000 system (Biacore AB, Uppsala, Sweden) was used for SPR analysis. The N-terminally biotinylated peptides APC and RIL (KRHSGSYLVTSV$_{COOH}$ and VAVYPNAKVELV$_{COOH}$, respectively; Ansynth Service B.V., Roosendaal, The Netherlands) were loaded onto streptavidin (SA)-coated sensor chips at a flow rate of 5 μL/min using the manufacturer's instructions. Purified GST fusion proteins, or GST alone as a control, were dialyzed against running buffer (10 mM Hepes, pH 7.4, 150 mM NaCl, 3 mM EDTA, 0.005% surfactant P20) and diluted to the concentrations indicated. Perfusion was at a flow rate of 25−50 μL/min, first over a control flow cell coated with biotin (Fc1) and then over capture flow cells coated with the biotinylated peptides (Fc2−4). After 6−8 min of association, the sample solution was replaced by running buffer alone, allowing the complex to dissociate. Binding was measured as the difference between the Fc1 and Fc2−Fc4 curves. The binding surface was regenerated with two 60 s pulses of glycine, pH 2.0. Experiments were performed at 25 °C. Association and dissociation kinetics were fitted using a two independent site model as implemented in the Prism 4.0 program (GraphPad Software, Inc.). Binding curves consisted of a fast and a slow process, the latter of which appeared concentration-independent and may reflect GST dimerization or other modulating effects. Dissociation constants were derived from a concentration-dependent series.

NMR Measurements. NMR samples contained ∼1 mM uniformly labeled ^{15}N/^{13}C PDZ2 protein in a buffer consisting of 50 mM KH_2PO_4/K_2HPO_4 and 50 mM KCl, pH 6.8, H_2O/D_2O (95%/5%), and a trace amount of NaN_3 (*21*). Unlabeled peptide corresponding to the RIL (VAVYPNAKVELV) C-terminus was titrated into the PDZ2 domain-containing sample until the ^{15}N HSQC spectra of PDZ2 showed little further changes, with final peptide concentrations of 2.4 mM. All NMR experiments were recorded at 25 °C. The sequential assignments were completed using 3D HNCA and CCH-TOCSY experiments recorded on either a Varian Inova 500 or a Varian Inova 600 spectrometer. All spectra were processed using the NMRPipe program suite (*22*) and assigned using XEASY (*23*). The RIL assignments have been deposited in the BioMagResBank under accession number 6091. Freeze-dried, unlabeled PDZ1 was added to a 0.5 mM solution of uniformly ^{15}N-labeled PDZ2 in phosphate buffer, as described above. Relative concentrations of PDZ1 and PDZ2 were checked by 1D ^{15}N-edited/filtered experiments. ^{15}N HSQC spectra of PDZ2 were recorded at PDZ1:PDZ2 ratios of 0:1, 0.6:1, 1:1, 1.2:1, and 1.6:1.

Model Building of the PDZ2−RIL Peptide. The lowest energy structure of the PDZ2−APC complex (PDB code 1VJ6; *17*) was used as the starting point for building the model using the program Yasara Dynamics (http://www.yasara.org). First, the APC peptide was mutated to the corresponding residues of the RIL peptide. Immediate steric clashes of the side chains were removed by rotation or small displacement of the peptide. Next, with the protein conformation fixed, a short simulated annealing run in water using the AMBER99 force field optimized the peptide conformation. In two successive simulated annealing runs in water, increasing conformational freedom was introduced by first allowing also the protein residues lining the binding pocket to adjust, followed by a complete freedom for all residues of the complex. In each of these two steps, the variability of the conformation was examined by manual adjustment of side chain rotamers and/or small adjustments of the atomic positions of peptide residues. The overall side chain orientation and H-bond formation were typically reproduced from these different situations.

RESULTS

Identification of PTP-BL PDZ Interacting Peptides. To allow a comparison of the carboxyl terminal target specificity of PTP-BL PDZ domains individually or in clusters, we first screened a random C-terminal nonapeptide λ phage display library using GST-tagged individual PTP-BL PDZ domains bound to glutathione−Sepharose 4B beads as an affinity matrix. Peptides exposed on phages that were obtained after three successive selection cycles were aligned with respect to their carboxyl terminus, which led to consensus binding

A

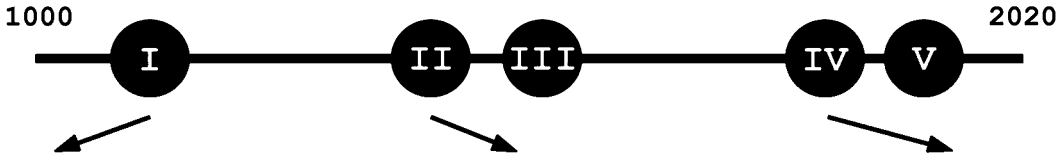

Class I
2 R R A F C G **S** **W** **V**
3 T V Q F C G **S** **W** **V**
4 E W V R Q S **T** **W** **V**
5,6 A R D q T C **T** **W** **V**
7,8 V S S C T G **T** **W** **V**
consensus: [S/T]WV

Unclassified
1 Q V M R G Y G **W** **V**

Class I
5 N S P D G G **S** Q **V**
8 K S I E V S **S** F **L**
21 G C Q G Y L **S** E **V**
18 W S A V E Q **S** F **L**
consensus: Sx[V/L]

Class II
12 P A N D W L **L** S **F**
20 C R E L G M **A** L **V**
consensus: ΦxΦ

Class III
1 M C S C N W **E** I **V**
9 R S P M L Q **E** T **V**
consensus: ExV

Unclassified
11 V V D S A E G L **V**
13 S W V G G E H I **V**

Class I
5 L V G S D V **T** F **L**

Class II
4 S Y G P E V **I** S **V**

Class III
1,3, A A A K E F **E** A **V**
6,7-10

Unclassified
2 L E W D I K Y D **V**

B

PDZ1 target proteins:		
BP75	-PDAS	**U**
IκBα	ankyrin repeat	**U**

PDZ2 target proteins:		
p75	-TSPV	**I**
hFAS	-QSLV	**I**
TRIP6	-TTDC	**I**
APC	-VTSV	**I**
RIL	-VELV	**III**

PDZ4 target proteins:		
EphrinB	-YYKV	**II**
RIL	-VELV	**III**
PARG1	-PQFV	**U**
CRIP2	LIM domain	**U**

FIGURE 1: C-terminal peptides selected by PTP-BL PDZ domains. (A) On top, a schematic representation of the relevant segment of PTP-BL (positions 1000−2020; accession no. Q64512) is shown, comprising its five PDZ domains. Below, the C-terminal sequence encoded by each phage clone selected by the indicated PDZ domain is shown. PDZ5 of PTP-BL did not yield specifically selected phage clones. Results for PTP-BL PDZ3 have been published elsewhere (*25*). Clone numbers are depicted in bold on the left, and peptides are classified according to Vaccaro et al. (*6*). Conserved residues (defined as appearing in more than 50% of the peptides) are depicted in bold and are represented in the consensus that is shown in bold and italic. The single-letter code for amino acids is used, Φ represents residues with hydrophobic side chains, and x represents any amino acid. (B) The currently reported interacting proteins for the individual PTP-BL PDZ domains are listed. Their four C-terminal amino acid residues are shown, and peptide classification (*6*) is indicated on the right. The PDZ target sequences in I*κ*Bα and CRIP2 are noncanonical, being the ankyrin repeats and LIM domains, respectively (*24*, *35*).

motifs for the different PTP-BL PDZ domains (Figure 1). In this assay, PDZ1 displayed an exclusive preference for class I peptides (ending with -(S/T)xΦ, where x denotes any amino acid and Φ hydrophobic residues (*4*)) that carry a tryptophan residue at the P^{-1} position. PTP-BL PDZ2 and PDZ4 both selected phages expressing C-terminal peptides that belong to class I, II (ending in -(Φ/Ψ)xΦ, where Ψ denotes aromatic residues (*4*)), or III (-G(D/E)xV (*4*)). This finding corresponds well with the diversity in C-terminal tails of reported interacting proteins (*8*, *24*). PDZ5 did not selectively bind peptide-displaying phages, and results obtained for PDZ3 have been described previously (*25*).

PDZ1 Alters PDZ2 Binding Specificity. To investigate whether PTP-BL PDZ domain binding preferences depend on intramolecular interactions, we tested several combinations of PDZ domains in phage display experiments. Intriguingly, a protein segment spanning the first two PDZ domains of PTP-BL (PDZ1+2) failed to select phage clones expressing class III peptides, while class I peptide-displaying phages were readily obtained (Figure 2A), which is in sharp contrast to results obtained for PDZ2 alone (Figure 1). SPR experiments confirmed these results: PDZ1+2 readily bound to the class I peptide (Figure 2B), while an interaction with a class III peptide was hardly detectable (Figure 2C). This modulation of PDZ2 domain preference is specific for PDZ1+2 because a segment spanning PTP-BL PDZ domains 4 and 5 (PDZ4+5) did not reveal an altered binding preference for PDZ4 in phage display and SPR experiments. Phage display screening using the PDZ4+5 fusion construct yielded phages expressing peptide classes II and III (Figure 2A), much like for PDZ4 alone. Likewise, the PDZ4+5 combination was still capable of binding to the class III RIL peptide in SPR experiments (Figure 2C).

PDZ1 Binds Directly to PDZ2. The observed difference in binding specificity of PDZ1+2 in comparison to PDZ2 alone suggests either a direct interaction between the two PDZ domains or an effect caused by the ∼200 amino acid long spacer region separating these domains. We therefore produced a GST-PDZ1+2 variant lacking the spacer sequence and tested its binding characteristics by SPR (data

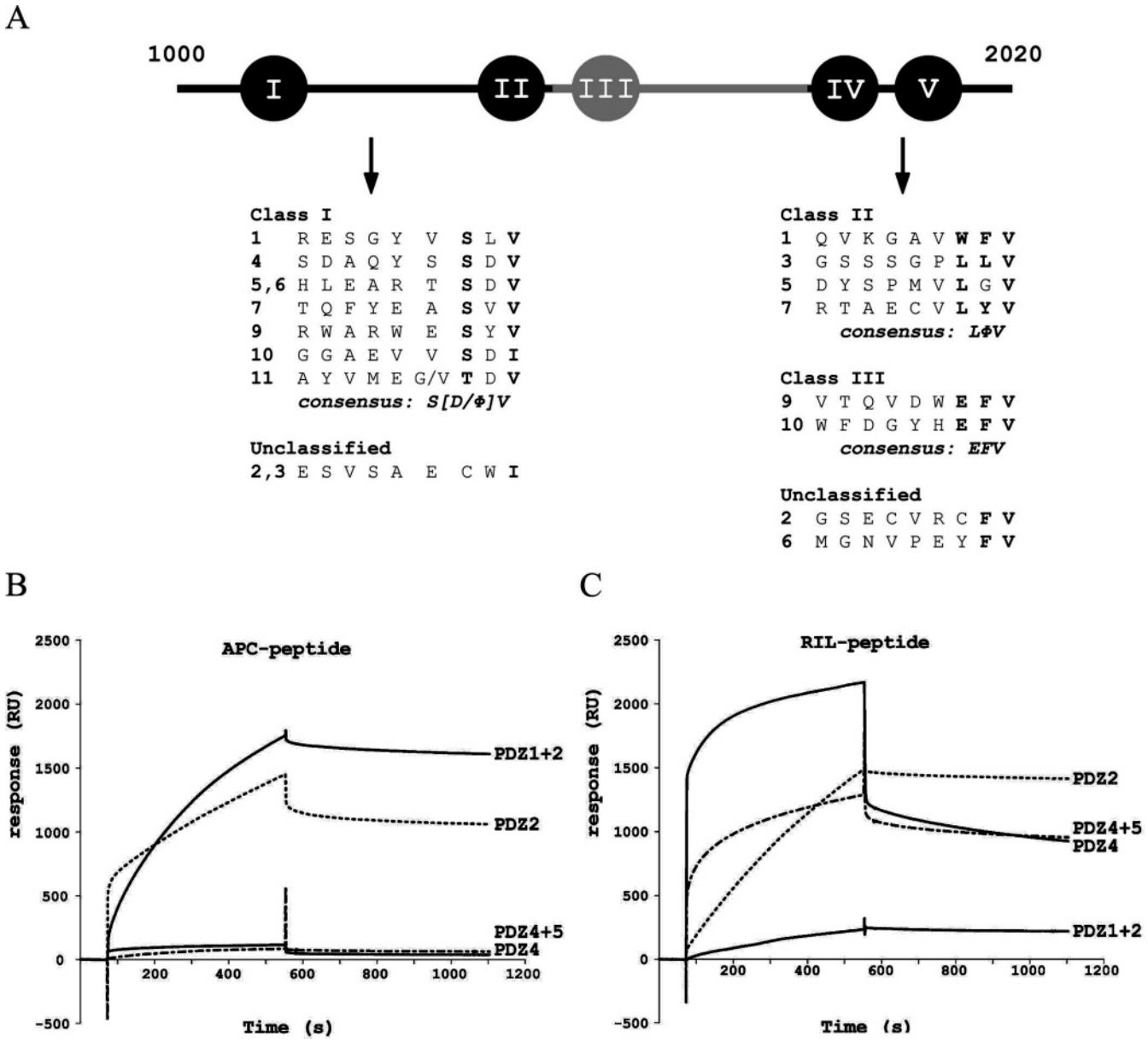

FIGURE 2: Peptide binding specificity of two PTP-BL PDZ domain combinations. (A) On top, a schematic representation of the relevant segment of PTP-BL, comprising the PDZ domain combinations PDZ1+2 and PDZ4+5, is depicted. Below, the C-terminal sequence encoded by each phage clone selected by the respective combination is shown. Clone numbers are depicted in bold on the left. Peptides were classified according to Vaccaro et al. (*6*). Conserved residues (defined as appearing in more than 50% of the peptides) are depicted in bold and are represented in the consensus that is shown in bold and italic. The single-letter code for amino acids is used, Φ represents residues with hydrophobic side chains, and x represents any amino acid. (B, C) Different combinations of PTP-BL PDZ domains were screened for interaction using SPR. N-terminally biotinylated APC (B) and RIL (C) C-terminal peptides were loaded onto streptavidin-coated sensor chips and tested for interaction with the GST−PDZ fusion proteins indicated on the right. The response (resonance units, RU) to each fusion protein is depicted (on the *y* axis) against time (s; *x* axis).

not shown). The PDZ1+2ΔL fusion, like GST-PDZ1+2, was found to readily bind APC but hardly RIL peptides, eliminating the spacer and pointing to PDZ1 as the modulator of PDZ2 binding preference. Several examples of PDZ−PDZ interactions have previously been reported (*26*−*29*). Hence, we tested the possibility of a direct interaction by titrating unlabeled PDZ1 into a sample containing ^{15}N-labeled PDZ2 for which the ^{15}N HSQC spectrum has been assigned (*21*). This allowed the direct mapping of the PDZ1−PDZ2 interaction interface on the PDZ2 structure. Upon addition of PDZ1, major shifts were observed for signals of PDZ2 residues present in α1 and β1 and the C-terminal tip of β6, jointly forming a surface opposite the C-terminal peptide binding groove (Figure 3A). Changes were also observed for Gly-26 and Arg-86, two residues present at the top of the canonical binding groove that play a crucial role in PDZ target binding, indicating that long-range allosteric effects caused by PDZ1 binding to the opposite side of the PDZ2 domain may well alter the binding preference of PDZ2. Importantly, there were no shifts observed for the ^{15}N−^{1}H PDZ2 resonances when the second PDZ domain of the neuronal adaptor X11α (*30*) was added to a ^{13}C/^{15}N-labeled sample (data not shown), underscoring the specificity of the PTP-BL PDZ1−PDZ2 interaction.

Structural Analysis of PTP-BL PDZ2 in Complex with a Class III Peptide. The observed PTP-BL PDZ2 binding promiscuity toward C-terminal targets (Figure 1; *8*) and the abrogation of class III peptide binding in response to PDZ1

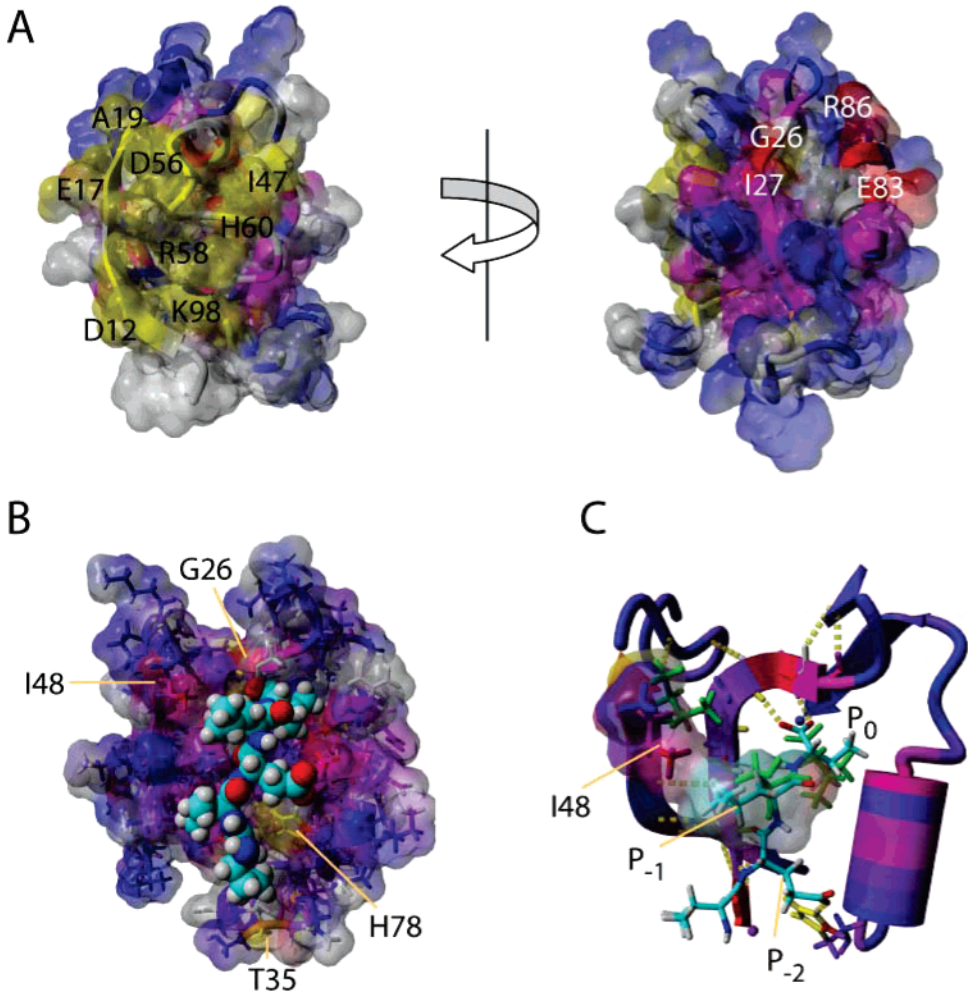

FIGURE 3: (A) van der Waals surface representation of the structure of the PDZ2 domain. Color coded according to the effects observed in the ^{15}N HSQC spectra upon titration of the PDZ1 domain: gray, no data; blue, no effects observed; purple, small changes; red, large changes; yellow, large effects indicative of slow chemical exchange. The second orientation is obtained by rotation of ~180° along the vertical axis. Relevant amino acid residues are indicated. (B) Model of the PDZ2−RIL complex. PDZ2 is shown in van der Waals surface representation and as sticks, color-coded as a ramp from blue to yellow, reflecting no to large chemical shift changes observed between the complex and native states. The RIL peptide is displayed in CPK representation. The most affected PDZ2 residues are indicated. (C) Peptide binding regions of the PDZ2−RIL model (color coded as in (B)) and PDZ2−APC complex structure (green). van der Waals surfaces of PDZ2 Ile-48 and RIL P^{-1} Leu are shown; selected H-bonds are displayed as yellow dotted lines. All figures were made using YASARA (http://www.yasara.org), and residue numbering was according to ref *21*.

association urged us to investigate the structural determinants allowing this discriminatory effect. We therefore determined the ^1H, ^{13}C, and ^{15}N chemical shifts of the PDZ2−RIL peptide complex by high-resolution triple-resonance NMR and compared these to the values of the native PDZ2. To establish the correlation between observed chemical shift differences in PDZ2 and structural effects resulting from peptide binding, we also examined the PDZ2−APC complex in comparison to the native PDZ2, for which both near complete assignments and structural ensembles are available in both states (*17*, *21*). The chemical shift differences observed for the PDZ2−RIL complex clearly indicated that the RIL peptide inserted into the canonical PDZ domain binding pocket located between helix α2 and strand β2 (cf. Figure 3B). Crucial chemical changes observed for the PDZ−APC complex involving Gly-26 and Leu-85 at the base of the binding pocket and Val-82 and Arg-86 at the C-terminal end of helix α2 were also observed for the PDZ2−RIL complex. Additionally, a contiguous stretch of affected residues lined the binding pocket of the PDZ2 domain. Interestingly, C^α, H^α, and C^β chemical shift changes for Ile-48 at the tip of the strand β3 were among the most extreme, indicating that this residue was in a more extended conformation. Moreover, large chemical shift changes of its C^δ−H^δ resonances indicate proximity of these atoms to the peptide. Such effects were not observed for Ile-48 in the case of the PDZ2−APC complex.

We next used the lowest energy conformer of the PDZ−APC structural ensemble (*17*) as a starting point to generate a model (cf. Figure 3B,C) for the PDZ2−RIL complex using Yasara (http://www.yasara.org). The peptide was easily accommodated within the PDZ2 binding pocket and explained remarkably well the key elements of the observed changes. The large effects at the base of the binding pocket and C-terminal end of helix α2, as observed for both the PDZ2−RIL and PDZ2−APC complexes, can be attributed to the interaction of the carboxyl-terminal (P^0) valine residue present in both peptides. PDZ2 Ile-48 is in van der Waals contact with the penultimate (P^{-1}) leucine residue of the RIL peptide. The side chain carboxyl group of P^{-2} Glu of the peptide hydrogen-bonded with His-78 located at the N-terminus of helix α2. Finally, P^{-4} Lys of the peptide

interacted with Thr-35 in the long loop connecting strands β2 and β3. Previous kinetic binding studies also showed Thr-35 to be important for PDZ2 target binding (*17*).

Quantitative Analysis of PTP-BL PDZ. C-Terminal Target Affinities. The interaction of the APC peptide with PDZ2 resulted overall in larger chemical shift differences when compared to that of RIL (data not shown), indicating a difference in affinity. We therefore determined the binding constants for the peptide−PDZ complexes in SPR measurements using biotinylated APC and RIL C-terminal peptides on streptavidin-coated sensor chips. As expected (*15*, *31*), PTP-BL PDZ2 bound to both peptides (class I and class III), whereas PDZ4 only interacted with the RIL peptide (Figure 4). The use of different concentrations of GST−PDZ fusion protein allowed the determination of the apparent dissociation constants (K_D) for the APC and RIL peptides toward PDZ2, 27 and 45 μM, respectively. This confirmed the suggested higher binding affinity of PDZ2 for the APC peptide as compared to RIL. PDZ4, however, displayed a higher affinity for the RIL C-terminal tail ($K_D = 21$ μM) than that of PDZ2. The apparent dissociation constants determined here are within the typical range observed for other PDZ domain interactions (*31*−*34*).

DISCUSSION

Over the past decade, attempts to understand, classify, and predict PDZ domain binding preferences were based on studies in which the target selection specificity was determined for individual PDZ domains in isolation. More recent studies, however, raise the concern that these results may be compromised due to this deterministic approach. Indeed, our current study demonstrates that the binding characteristics of one of the five PDZ domains in PTP-BL, PDZ2, is allosterically modulated by PTP-BL PDZ1, underscoring the notion that for a full appreciation of PDZ functioning long-range interactions should be taken into account.

Our unbiased determination of PTP-BL PDZ domain binding preferences, by screening a random C-terminal peptide phage display library using individual GST-tagged PDZ domains, revealed a binding consensus for domains PDZ2 and PDZ4 that nicely fitted with current knowledge on potential PTP-BL binding partners (reviewed in ref *8*). In contrast, we noted a clear preference of PDZ1 for class I peptides with a penultimate tryptophan residue, whereas reported PDZ1 interactions rather reflect binding to protein-internal ankyrin repeats (*35*) or to the carboxyl-terminal portion of a bromodomain-containing protein (*36*). For the latter interaction, the C-terminus appeared necessary but not sufficient for strong PDZ1 binding (*36*), reminiscent of the interaction between PTP-BL PDZ domains and the RIL C-terminus (*15*). The screening with PTP-BL PDZ3 yielded peptide targets containing cysteine residues at P^{-1} and P^{-4} and a valine at the ultimate P^0 position (*25*) and that did not resemble the C-terminal tail of its sole reported target, PRK2 (*37*). No specific peptide-displaying phages were selected by PTP-BL PDZ5, in accordance with results from alternative strategies (*8*). The only reported PDZ5 interaction thus far is with phosphatidylinositol 3,4-biphosphate, a phosphoinositide that also binds to PTP-BL PDZ2 and PDZ3 (*38*). Perhaps PTP-BL PDZ5 is not involved in target peptide binding but rather serves in modulating the structure of the

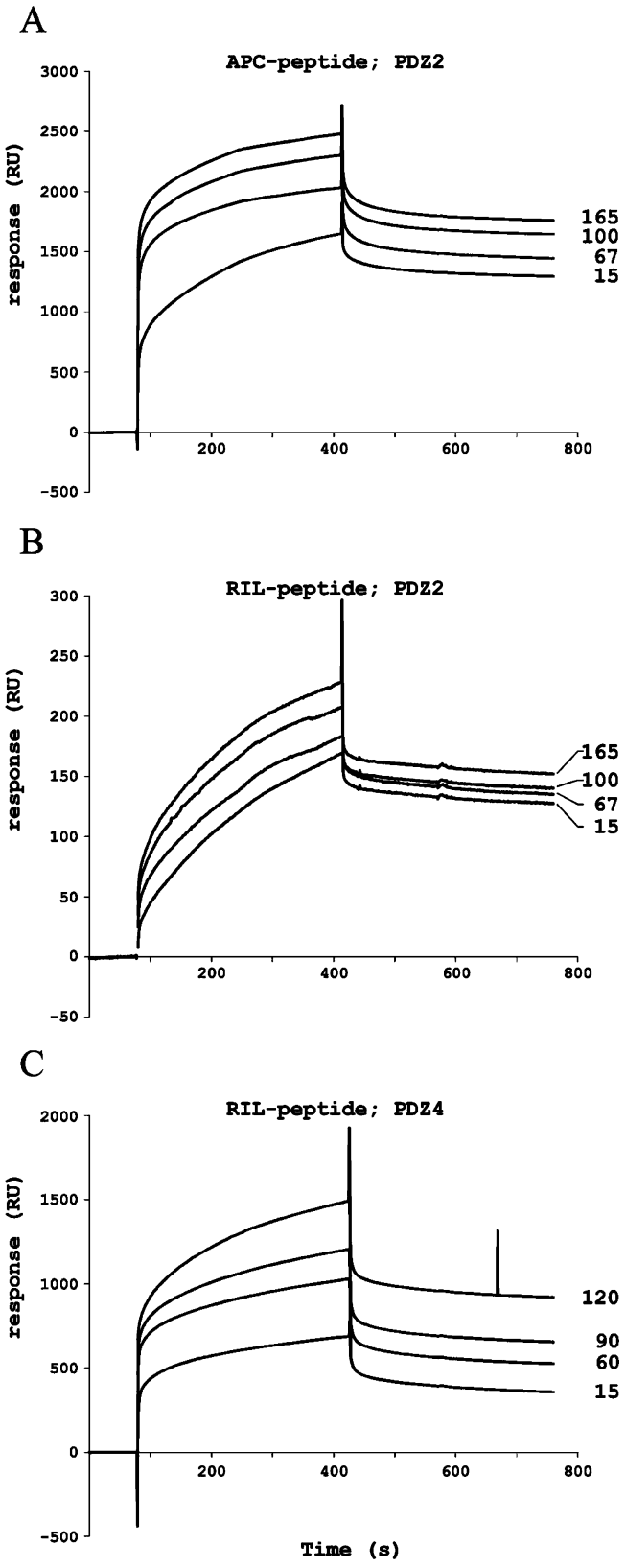

FIGURE 4: Biosensor analysis of PTP-BL PDZ domain interactions with APC and RIL C-termini. The binding of GST fusions of PTP-BL PDZ2 (A, B) or PDZ4 (C), at different concentrations (indicated on the right, μM), to the APC C-terminal peptide (A) or the RIL C-terminus (B, C) immobilized on the surface of a sensor chip was detected by changes in resonance units over time (s). The sensorgrams shown were obtained by subtracting the blank sensorgram of a control nonpeptide flow cell from the sensorgrams of the peptide-loaded cells.

adjacent proximal PDZ domain as observed for the glutamate receptor-interacting protein GRIP. PDZ4 in GRIP does not bind other proteins but instead stabilizes the closely linked PDZ5 domain, thereby allowing it to bind C-terminal targets (*9*). For PTP-BL, however, we did not detect such an effect of PDZ5 on the binding characteristics of the neighboring PDZ4 domain (compare Figures 1 and 2).

PTP-BL PDZ domains 2 and 4 displayed the most promiscuity, having interactions with a rather diverse set of peptides from various classes (Figure 1). The current structural comparison of PDZ2 in complex with a class I (APC) or a class III (RIL) C-terminal ligand revealed that these interactions both exploit the canonical binding groove. Figure 3C shows the peptide binding region of both the PDZ2−RIL model and the PDZ2−APC complex. The common orientation of the P^0 Val residue of both peptides is evident, in line with the highly similar patterns of chemical shift differences observed for both complexes. However, the RIL P^{-1} Leu residue is in direct van der Waals contact with Ile-48, thereby displacing this residue relative to that of the PDZ2−APC complex. In the latter, this residue is not involved in peptide binding. Traditional classification schemes of PDZ domain interactions primarily involve the characteristics of the terminal and antepenultimate residues (P^0 and P^{-2}) of the peptide ligand and regard the P^{-1} residue as "functionally unimportant and poorly conserved" (*39*). However, classification schemes based on peptide sequence alone are incapable of explaining many observed PDZ−target interactions, including the promiscuous ones as observed for PDZ2. A more recent model, prompted by the observation that PDZ2 syntenin bound different ligands through interactions involving either the P^0 and P^{-1} residues or the P^0 and P^{-2} residues (*40*), postulates that ligands bind in a combinatorial fashion to multiple smaller "sites" in PDZ domains. The binding promiscuity of the PTP-BL PDZ2 domain is in full concordance with such a model and underscores a crucial differentiating role for Ile-48 through its interaction with the P^{-1} residue in class III targets. In line with this, multiple sequence analyses show that PTP-BL PDZ2 Ile-48 is conserved throughout the vertebrate kingdom and also the promiscuous PTP-BL PDZ4 contains an isoleucine residue at the structurally equivalent position. Analysis of eight different PDZ domain−peptide crystal structures revealed that complexes involving P^{-1} interactions generally display reduced interaction surfaces as compared to those that do not involve the P^{-1} peptide residue (data not shown). The difference in affinity as observed in the SPR measurements for the APC peptide relative to the RIL peptide (Figure 4) is in line with such a difference in peptide interaction surfaces. Furthermore, it provides an explanation for the requirement of the RIL LIM domain to elicit efficient in vivo binding (*15*).

In many proteins that harbor multiple PDZ domains, such as PTP-BL, a conspicuous clustered appearance of these domains is apparent. Three-dimensional structures for several different PDZ tandems have been solved, revealing that the PDZ domain orientation in such tandems varies considerably (*9*−*11*). For instance, the PSD-95 PDZ domain tandem displayed limited rotational freedom, and the respective peptide binding grooves appeared aligned, explaining their tendency to interact with dimeric ligands (*11*). The two syntenin PDZ domains, on the other hand, displayed independent and fully solvent-accessible peptide binding pockets (*10*). In contrast, GRIP PDZ domains 4 and 5 were rather tightly packed together, which stabilized the PDZ5 structure but caused a distorted peptide binding groove within PDZ4 that may preclude binding of C-terminal peptides (*9*). We examined the target specificity of PTP-BL PDZ domain clusters and found, in line with proposed allosteric effects based on structural analyses of PDZ2−ligand complexes (*17*−*19*), that the PDZ2 binding specificity as observed in isolation is modulated by PDZ1 as a result of a direct and specific, probably electrostatic, interaction of PDZ1 with the $\alpha1-\beta1$ interface on PDZ2. Importantly, PDZ1 binding affected crucial residues in the PDZ2 peptide binding groove on the opposite side of the domain, consistent with the rather flexible, adaptive character of PDZ2 as displayed in kinetic folding studies (*41*) and the long-range effects observed in PDZ2−peptide complexes (*17*−*19*). Moreover, structural coupling between these two parts of PDZ domains has also been inferred from theoretical calculations (*42*).

How then would the PDZ1 binding alter the specificity of the PDZ2 domain toward the class I group of targets, as both class I and class III involve interactions in the P^0 and P^{-2} binding pockets? We hypothesize that the PDZ1−PDZ2 association renders PDZ2 incapable of adjusting for the required Ile-48−P^{-1} interaction (Figure 3C). Structural adjustments have also been noted for the binding process, leading to the PDZ2−APC complex, which first involves an association of the APC P^0 residue with the PDZ domain, followed by a structural rearrangement of the latter that locks the interaction into place (*17*). Interestingly, Ile-47, which just precedes Ile-48 and is structurally connected to helix $\alpha1$, is among the residues highly affected by the PDZ1−PDZ2 interaction (Figure 3A). The loss of the P^{-1} interaction would then be paramount for the loss of affinity of the RIL target, whereas the APC target is not affected and could even be boosted by a structural change of PDZ2 toward a high-affinity conformation. Such structural changes in the binding pocket appear to be an important regulatory factor, as evident from the formation of the PDZ2−APC complex (*17*) and the loss of affinity by the alternatively spliced PDZ2 (*43*). An allosteric transition has also been documented for Par-6 (*44*, *45*), where a CRIB (Cdc42/Rac interactive binding) domain that precedes its single PDZ domain in fact forms an extension of the central PDZ domain β-sheet. Cdc42 binding to the Par-6 CRIB domain subsequently boosts the affinity of the flanking PDZ domain for its C-terminal ligand (*44*, *45*). Interestingly, the Par-6 PDZ residues that are contacted by the CRIB domain are structurally similar to those in PTP-BL PDZ2 that are affected by PDZ1. Such PDZ−PDZ interactions provide an excellent means to regulate ligand binding specificity and may well form the basis of the conspicuous coappearance of PDZ domains in signaling and scaffolding proteins.

ACKNOWLEDGMENT

We thank J. Aelen, J. Schepens, M. Fabbri, and G. De Matienzo for excellent technical support, M. Ubbink and A. Blok for providing the ^{15}N-labeled X11α PDZ2 recombinant protein, and E. Lasonder and W. Roeffen for help in using the BIAcore 2000 system.

REFERENCES

1. Pawson, T., and Nash, P. (2003) Assembly of cell regulatory systems through protein interaction domains, *Science 300*, 445−452.
2. van Ham, M., and Hendriks, W. (2003) PDZ domains−glue and guide, *Mol. Biol. Rep. 30*, 69−82.
3. Nourry, C., Grant, S. G., and Borg, J. P. (2003) PDZ domain proteins: plug and play!, *Sci. STKE 2003*, RE7.
4. Vaccaro, P., Brannetti, B., Montecchi-Palazzi, L., Philipp, S., Citterich, M. H., Cesareni, G., and Dente, L. (2001) Distinct binding specificity of the multiple PDZ domains of INADL, a human protein with homology to INAD from Drosophila melanogaster, *J. Biol. Chem. 276*, 42122−42130.
5. Songyang, Z., Fanning, A. S., Fu, C., Xu, J., Marfatia, S. M., Chishti, A. H., Crompton, A., Chan, A. C., Anderson, J. M., and Cantley, L. C. (1997) Recognition of unique carboxyl-terminal motifs by distinct PDZ domains, *Science 275*, 73−77.
6. Vaccaro, P., and Dente, L. (2002) PDZ domains: troubles in classification, *FEBS Lett. 512*, 345−349.
7. Hendriks, W., Schepens, J., Bächner, D., Rijss, J., Zeeuwen, P., Zechner, U., Hameister, H., and Wieringa, B. (1995) Molecular cloning of a mouse epithelial protein-tyrosine phosphatase with similarities to submembranous proteins, *J. Cell. Biochem. 59*, 418−430.
8. Erdmann, K. S. (2003) The protein tyrosine phosphatase PTP-Basophil/Basophil-like; Interacting proteins and molecular functions, *Eur. J. Biochem. 270*, 4789−4798.
9. Feng, W., Shi, Y., Li, M., and Zhang, M. (2003) Tandem PDZ repeats in glutamate receptor-interacting proteins have a novel mode of PDZ domain-mediated target binding, *Nat. Struct. Biol. 10*, 972−978.
10. Kang, B. S., Cooper, D. R., Jelen, F., Devedjiev, Y., Derewenda, U., Dauter, Z., Otlewski, J., and Derewenda, Z. S. (2003) PDZ tandem of human syntenin. Crystal structure and functional properties, *Structure (London) 11*, 459−468.
11. Long, J. F., Tochio, H., Wang, P., Fan, J. S., Sala, C., Niethammer, M., Sheng, M., and Zhang, M. (2003) Supramodular structure and synergistic target binding of the N-terminal tandem PDZ domains of PSD-95, *J. Mol. Biol. 327*, 203−214.
12. Grootjans, J. J., Reekmans, G., Ceulemans, H., and David, G. (2000) Syntenin-syndecan binding requires syndecan-synteny and the co-operation of both PDZ domains of syntenin, *J. Biol. Chem. 275*, 19933−19941.
13. Raghuram, V., Mak, D. D., and Foskett, J. K. (2001) Regulation of cystic fibrosis transmembrane conductance regulator single-channel gating by bivalent PDZ-domain-mediated interaction, *Proc. Natl. Acad. Sci. U.S.A. 98*, 1300−1305.
14. Jannatipour, M., Dion, P., Khan, S., Jindal, H., Fan, X., Laganiere, J., Chishti, A. H., and Rouleau, G. A. (2001) Schwannomin isoform-1 interacts with syntenin via PDZ domains, *J. Biol. Chem. 276*, 33093−33100.
15. van den Berk, L., van Ham, M., te Lindert, M. M., Walma, T., Aelen, J., Vuister, G. W., and Hendriks, W. J. A. J. (2004) The interaction of PTP-BL PDZ domains with RIL: An enigmatic role for the RIL LIM domain, *Mol. Biol. Rep. 31*, 203−215.
16. Cuppen, E., Gerrits, H., Pepers, B., Wieringa, B., and Hendriks, W. (1998) PDZ motifs in PTP-BL and RIL bind to internal protein segments in the LIM domain protein RIL, *Mol. Biol. Cell 9*, 671−683.
17. Gianni, S., Walma, T., Arcovito, A., Calosci, N., Bellelli, A., Engstrom, A., Travaglini-Allocatelli, C., Brunori, M., Jemth, P., and Vuister, G. W. (2006) Demonstration of long-range interactions in a PDZ domain by NMR, kinetics, and protein engineering, *Structure (London) 14*, 1801−1809.
18. Fuentes, E. J., Gilmore, S. A., Mauldin, R. V., and Lee, A. L. (2006) Evaluation of energetic and dynamic coupling networks in a PDZ domain protein, *J. Mol. Biol. 364*, 337−351.
19. Fuentes, E. J., Der, C. J., and Lee, A. L. (2004) Ligand-dependent dynamics and intramolecular signaling in a PDZ domain, *J. Mol. Biol. 335*, 1105−1115.
20. Frangioni, J. V., and Neel, B. G. (1993) Solubilization and purification of enzymatically active glutathione S-transferase (pGEX) fusion proteins, *Anal. Biochem. 210*, 179−187.
21. Walma, T., Spronk, C. A. E. M., Tessari, M., Aelen, J., Schepens, J., Hendriks, W., and Vuister, G. W. (2002) Structure, dynamics and binding characteristics of the second PDZ domain of PTP-BL, *J. Mol. Biol. 316*, 1101−1110.
22. Delaglio, F., Grzesiek, S., Vuister, G. W., Zhu, G., Pfeifer, J., and Bax, A. (1995) NMRPipe: a multidimensional spectral processing system based on UNIX pipes, *J. Biomol. NMR 6*, 277−293.
23. Bartels, C. H., Xia, T.-H., Billeter, M., Guntert, P., and Wuthrich, K. (1995) The program XEASY for computer-supported NMR spectral analysis of biological macromolecules, *J. Biomol. NMR 6*, 1−10.
24. van Ham, M., Croes, H., Schepens, J., Fransen, J., Wieringa, B., and Hendriks, W. (2003) Cloning and characterization of mCRIP2, a mouse LIM-only protein that interacts with PDZ domain IV of PTP-BL, *Genes Cells 8*, 631−644.
25. van den Berk, L. C. J., Landi, E., Harmsen, E., Dente, L., and Hendriks, W. J. A. J. (2005) Redox-regulated affinity of the third PDZ domain in the phosphotyrosine phosphatase PTP-BL for cysteine-containing target peptides, *FEBS J. 272*, 3306−3316.
26. Xu, X.-Z. S., Choudhury, A., Li, X., and Montell, C. (1998) Coordination of an array of signaling proteins through homo- and heteromeric interactions between PDZ domains and target proteins, *J. Cell Biol. 142*, 545−555.
27. Fouassier, L., Yun, C. C., Fitz, J. G., and Doctor, R. B. (2000) Evidence for ezrin-radixin-moesin-binding phosphoprotein 50 (EBP50) self-association through PDZ-PDZ interactions, *J. Biol. Chem. 275*, 25039−25045.
28. Srivastava, S., Osten, P., Vilim, F. S., Khatri, L., Inman, G., States, B., Daly, C., DeSouza, S., Abagyan, R., Valtschanoff, J. G., Weinberg, R. J., and Ziff, E. B. (1998) Novel anchorage of GluR2/3 to the postsynaptic density by the AMPA receptor-binding protein ABP, *Neuron 21*, 581−591.
29. Im, Y. J., Lee, J. H., Park, S. H., Park, S. J., Rho, S. H., Kang, G. B., Kim, E., and Eom, S. H. (2003) Crystal structure of the Shank PDZ-ligand complex reveals a class I PDZ interaction and a novel PDZ-PDZ dimerization, *J. Biol. Chem. 278*, 48099−48104.
30. Duquesne, A. E., Ruijter, M., Brouwer, J., Drijfhout, J. W., Nabuurs, S. B., Spronk, C. A., Vuister, G. W., Ubbink, M., and Canters, G. W. (2005) Solution structure of the second PDZ domain of the neuronal adaptor X11alpha and its interaction with the C-terminal peptide of the human copper chaperone for superoxide dismutase, *J. Biomol. NMR 32*, 209−218.
31. Erdmann, K. S., Kuhlmann, J., Lessmann, V., Hermann, L., Eulenburg, V., Müller, O., and Heumann, R. (2000) The adenomatous polyposis coli-protein (APC) interacts with the protein tyrosine phosphatase PTP-BL via an alternatively spliced PDZ domain, *Oncogene 19*, 3894−3901.
32. Marfatia, S. M., Morais-Cabral, J. H., Kim, A. C., Byron, O., and Chishti, A. H. (1997) The PDZ domain of erythrocyte p55 mediates its binding to the cytoplasmic carboxyl terminus of glycophorin C, *J. Biol. Chem. 272*, 24191−24197.
33. Kim, E., DeMarco, S. J., Marfatia, S. M., Chishti, A. H., Sheng, M., and Strehler, E. E. (1998) Plasma membrane Ca2+ ATPase isoform 4b binds to membrane-associated guanylate kinase (MAGUK) proteins via their PDZ (PSD-95/Dlg/ZO-1) domains, *J. Biol. Chem. 273*, 1591−1595.
34. Miyagi, Y., Yamashita, T., Fukaya, M., Sonoda, T., Okuno, T., Yamada, K., Watanabe, M., Nagashima, Y., Aoki, I., Okuda, K., Mishina, M., and Kawamoto, S. (2002) Delphilin: a novel PDZ and formin homology domain-containing protein that synaptically colocalizes and interacts with glutamate receptor delta 2 subunit, *J. Neurosci. 22*, 803−814.
35. Maekawa, K., Imagawa, N., Naito, A., Harada, S., Yoshie, O., and Takagi, S. (1999) Association of protein-tyrosine phosphatase PTP-BAS with the transcription-factor-inhibitory protein IκBα through interaction between the PDZ1 domain and ankyrin repeats, *Biochem. J. 337*, 179−184.
36. Cuppen, E., van Ham, M., Pepers, B., Wieringa, B., and Hendriks, W. (1999) Identification and molecular characterization of BP75, a novel bromodomain-containing protein, *FEBS Lett. 459*, 291−298.
37. Gross, C., Heumann, R., and Erdmann, K. S. (2001) The protein kinase C-related kinase PRK2 interacts with the protein tyrosine phosphatase PTP-BL via a novel PDZ domain binding motif, *FEBS Lett. 496*, 101−104.
38. Zimmermann, P., Meerschaert, K., Reekmans, G., Leenaerts, I., Small, J. V., Vandekerckhove, J., David, G., and Gettemans, J. (2002) PIP(2)-PDZ domain binding controls the association of syntenin with the plasma membrane, *Mol. Cell 9*, 1215−1225.
39. Doyle, D. A., Lee, A., Lewis, J., Kim, E., Sheng, M., and MacKinnon, R. (1996) Crystal structures of a complexed and

peptide-free membrane protein-binding domain: molecular basis of peptide recognition by PDZ, *Cell 85*, 1067−1076.

40. Kang, B. S., Cooper, D. R., Devedjiev, Y., Derewenda, U., and Derewenda, Z. S. (2003) Molecular roots of degenerate specificity in syntenin's PDZ2 domain: reassessment of the PDZ recognition paradigm, *Structure (London) 11*, 845−853.
41. Gianni, S., Calosci, N., Aelen, J. M., Vuister, G. W., Brunori, M., and Travaglini-Allocatelli, C. (2005) Kinetic folding mechanism of PDZ2 from PTP-BL, *Protein Eng. Des. Sel. 18*, 389−395.
42. Lockless, S. W., and Ranganathan, R. (1999) Evolutionarily conserved pathways of energetic connectivity in protein families, *Science 286*, 295−299.
43. Walma, T., Aelen, J., Nabuurs, S., Oostendorp, M., van den Berk, L., Hendriks, W., and Vuister, G. W. (2004) A closed binding pocket and global destabilization modify the binding properties of an alternatively spliced form of the second PDZ domain of PTP-BL, *Structure (London) 12*, 11−20.
44. Garrard, S. M., Capaldo, C. T., Gao, L., Rosen, M. K., Macara, I. G., and Tomchick, D. R. (2003) Structure of Cdc42 in a complex with the GTPase-binding domain of the cell polarity protein, Par6, *EMBO J. 22*, 1125−1133.
45. Peterson, F. C., Penkert, R. R., Volkman, B. F., and Prehoda, K. E. (2004) Cdc42 regulates the Par-6 PDZ domain through an allosteric CRIB-PDZ transition, *Mol. Cell 13*, 665−676.

BI700954E